https://doi.org/10.48048/tis.2023.6403

Ensemble Pharmacophore Meets Molecular Docking: A Novel Screening Approach for the Identification of B-Raf Kinase Inhibitors

Muni Sireesha Sunkara[1], Vinutha Kuchana[1,*], Jyothi Vemuri[1] and Dipankar Bhowmik[2]

[1]Department of Pharmaceutical Chemistry, Sarojini Naidu Vanita Pharmacy Maha Vidyalaya, Tarnaka, Hyderabad 500017, India
[2]Associate Solution Leader, Brane Enterprises Pvt Ltd, Hyderabad, India

([*]Corresponding author's e-mail: vinutha_me@yahoo.co.in)

Received: 18 September 2021, Revised: 20 October 2021, Accepted: 28 October 2021, Published: 26 November 2022

Abstract

In US about 106110 diagnosed as melanomas, 7,180 people expected to die due to melanoma. B-RAF is a cytoplasmic serine - threonine kinase that is found in a mutated form in melanoma and colorectal cancer. Sorafenib was initially introduced as a B-RAF inhibitor in melanoma. Hence it is taken as a pivot molecule in our study. Four potent B-Raf kinase inhibitors (Sorafenib, Regorafenib, N-desmethyl sorafenib & Donafenib) are used to build a pharmacophore model with 'PharmaGist webserver' which generated a 5-point hypothesis. The best model with score of 27.780, was used to screen the Zinc database of ZINCPharmer web server to obtain similar pharmacophore hits. By applying filters like Lipinski rule, RMSD criteria in ZINCPharmer top ten hits were identified. Subsequently, molecular docking was performed on wild (1UWH) and mutated (3IDP) B-Raf kinase protein targets by using GLIDE 5.6 (Schrödinger), to prioritize top lead molecules. Further these molecules are subjected to ADME Properties Prediction by Qik Prop module. Among ten, nine molecules have glide scores in the range nearer to the standard molecule i.e., Sorafenib. Finally, we conclude that ZINC02853810 may act as a powerful inhibitor against both wild and mutant type B-Raf kinase as it has highest glide scores than the Standard.

Keywords: B-Raf kinase inhibitors, Pharmacophore modeling, PharmaGist, ZINCPharmer, ADME, Binding energy

Introduction

Cancer can be targeted by using agent's peculiar for regulating signaling pathways of cancer cells [1]. Melanoma is one among the most aggressive forms of skin cancer and a serious health issue worldwide because of its increasing incidence and the lack of satisfactory chemotherapy for the advanced stages of the disease [2,3]. It has a high ability of metastasis and rapid invasion of other organs, e.g., lymph node, lung, liver, brain, etc. [4]. In US about 106,110 diagnosed as melanomas, 7,180 people expected to die due to melanoma.

The Ras/Raf/MEK/Erk (MAPK) signaling pathway converts extracellular signals from cell membrane receptors to nuclear protein synthesis factors, thereby modulating fundamental cell processes like cellular amplification, differentiation, migration, growth, survival [5,6]. Ras is one of the specific proteins to be concentrated on. Ras (a membrane associated guanine nucleotide binding protein) will be triggered when it binds to an extracellular ligand. Ras proteins belong to a superfamily of low molecular weight GTP binding proteins [7]. A Protein, i.e., serine/threonine kinase Raf is the 1st mammalian direct effector of RAS. GTP-bound activated Ras binds and leads to activation of 3 intimately related RAF proteins named C-Raf, B-Raf, and A-Raf. This causes Raf to relocate to the plasma membrane, a prerequisite for its activity [8]. Raf (Rapidly accelerated fibrosarcoma) activation that can promote cell-cycle progression is identified as a downstream effector kinase of Ras [9]. The oncogene BRAF, as discovered in 1988 was thought to be responsible for 66 % of melanomas.

B-Raf is a mitochondrial protein having a molecular weight of 94kDa acts as a mutational target in various human cancers. Ras-Raf pathway is depicted in (**Figure 1**). The mutations in BRAF are present in approximately 2 % of human cancers, including particularly high frequencies 50 - 70 % of malignant melanomas and a lower frequency in a variety of other types of human cancers, such as thyroid (30 %), colorectal (10 %), and ovarian (35 %) cancers [10]. Melanomas show a high incidence of BRAF mutations and the most common mutation is a valine for glutamic acid substitution at position 600, termed

V600EBRAF which displays a permanent 500-fold elevated kinase activity [11]. V600EBRAF stimulates sustained and constitutive activation of the MAPK pathway, inducing uncontrolled cell proliferation, increased cell survival, and tumor progression. Almost 90 % of B-Raf mutations are the substitution of valine to glutamate residue 600(V600E) [12]. Since phosphorylation of Raf is considered a prerequisite in MAPK signaling pathway, pointing abnormal Raf became one of the desirable therapeutic targets and offering opportunities for anticancer drug development [13-15].

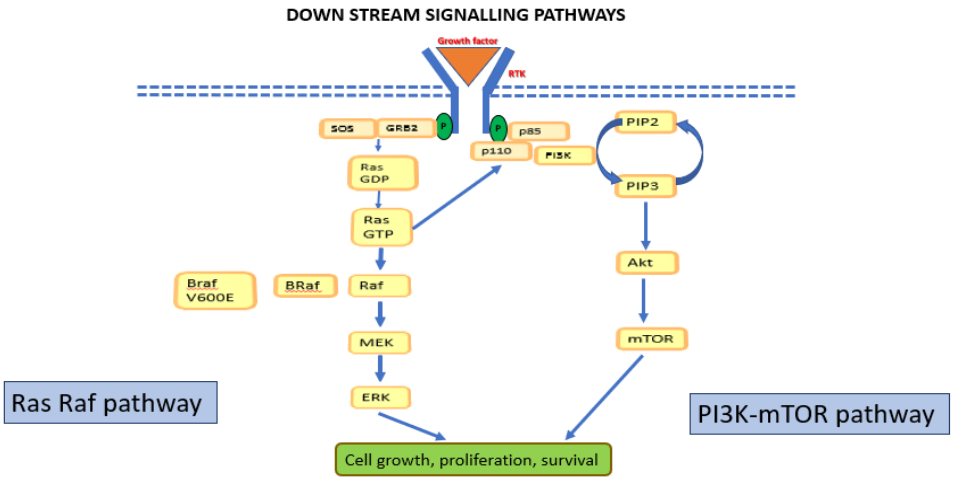

Figure 1 Ras-Raf pathway.

Many researchers reported several purinylpyridine and pyrimidine derivatives as B-Raf kinase inhibitors [16]. At present, some of the compounds which are under clinical trials (like PLX8394, RXDX105, MLN2480, LGX818, LY3009120) contained Pyrolopyridine, Pyrimidine, Pyridinyl pyrimidine cores which had potency invitro and in vivo against B-RafWTV600E attracted us to focus attention on them and to carry out further molecular modeling and 3D QSAR studies [16]. The Structures of B-Raf inhibitors under clinical trials are depicted in (**Figure 2**).

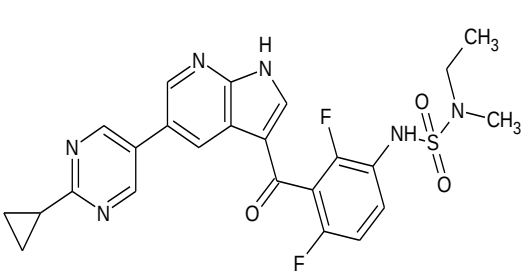

PLX8394

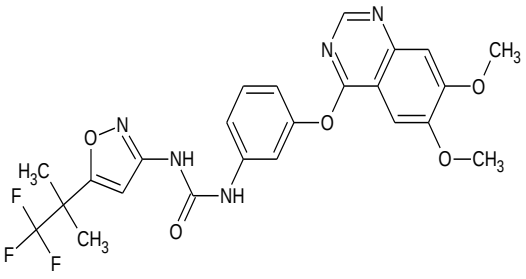

RXDX105

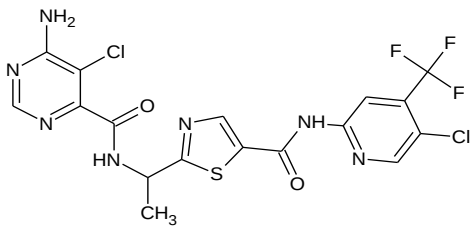

MLN2480(TAK580)

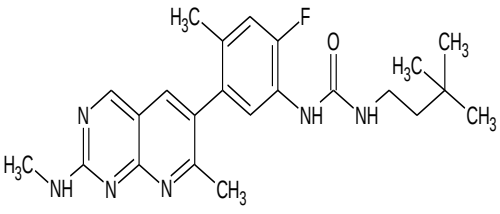

LY3009120

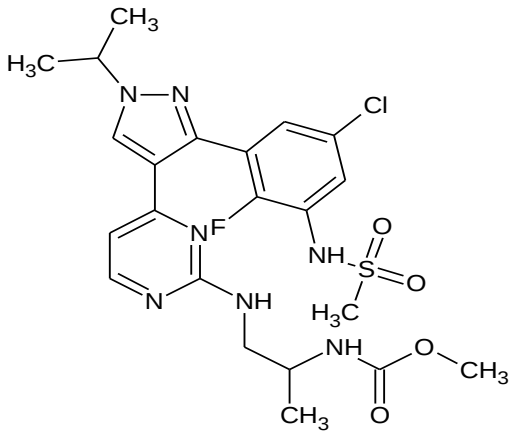

LGX818

Figure 2 The Structures of B-Raf inhibitors under clinical trials.

One of the important advancements in the design and discovery of new drugs was Molecular modeling (MM). At present, molecular modeling is considered as an indispensable tool in drug discovery and in optimizing existing prototypes and the rational design of drug candidates, of which virtual screening plays a pivotal role. At the outset, several protocols, such as development of a pharmacophore model, molecular dynamics, etc., have been established [17].

Ligand based pharmacophore method is used to develop pharmacophore model. The current research work encompasses various marketed or emerging B-Raf Kinase inhibitors traced by virtual screening on ZINCPharmer database to find potent B-Raf inhibitors.

The rationale of the concept is, molecules that share some structural similarity may have a similar activity. Some methods use known active ligands as a query inorder to extract structurally similar compounds from huge databases.

In present computational chemistry, the vital features of one or more ligands with same biological activity were well-defined using pharmacophore. It is defined as the 3-dimensional arrangement of features that is required for a ligand to interact with a specific target protein. These selected traits are substantial to accomplish best Pharmacophore Model. In the current research, we used PharmaGist, a web-based software to build a Pharmacophore model. It is a ligand-based method [18].

The screening process includes selection of best pharmacophore on ZINCPharmer Database and validated through the Docking studies.

Materials and methods

Target proteins

The crystal structures of 2 B-Raf kinase inhibitors (PDB IDS: 1UWH & 3IDP) were downloaded from the RCSB Protein data bank. Among the 2 protein targets 1UWH is the wild type and 3IDP is mutated i.e., B-Raf V600E. Both these have the crystal resolutions of 2.95 and 2.70 A^0, respectively.

Table 1 Crystal structures obtained from the RCSB protein data bank.

Protein	PDB ID	Confirmation	Phenotype	Resolution (A^0)	R-Value work	R-Value free
B-RAF	1UWH	DFG-ASP Out	Wild-type	2.95	0.222	0.222
	3IDP	DFG-ASP Out	Mutated	2.70	0.201	0.264

Ligand selection

The 3-dimensional structures of 4 selected ligands were retrieved from PubChem database in SDF format. Later they were viewed in Marvin view and saved in Tripos mol 2 format. Sorafenib was taken as a lead molecule which inhibits B-Raf kinase.

PharmaGist

The best open-source web server used for searching a pharmacophore using a set of ligands that bind to a target protein is PharmaGist. For every input ligand, this web server lists the number of atoms, 3 dimensional and physico-chemical features like hydrophobic regions, aromatic rings, hydrogen bond acceptors and hydrogen bond donors. This method expeditiously searches for all possible pharmacophores, generates 3-dimensional visualization of detected pharmacophore candidates by multiple flexible alignments of input ligands and executes virtual screening based on detected pharmacophore model [18].

ZINCPharmer

It is an Open-source web interface for searching biologically related molecules in the Zinc database (http://zincdocking.org/), consisting of over 22,724,825 molecules [18]. These were utilized for virtual screening process. The molecules which exhibited maximum similarity to query pharmacophore were filtered. Further, these hits were subjected to Lipinski rule of 5 filter.

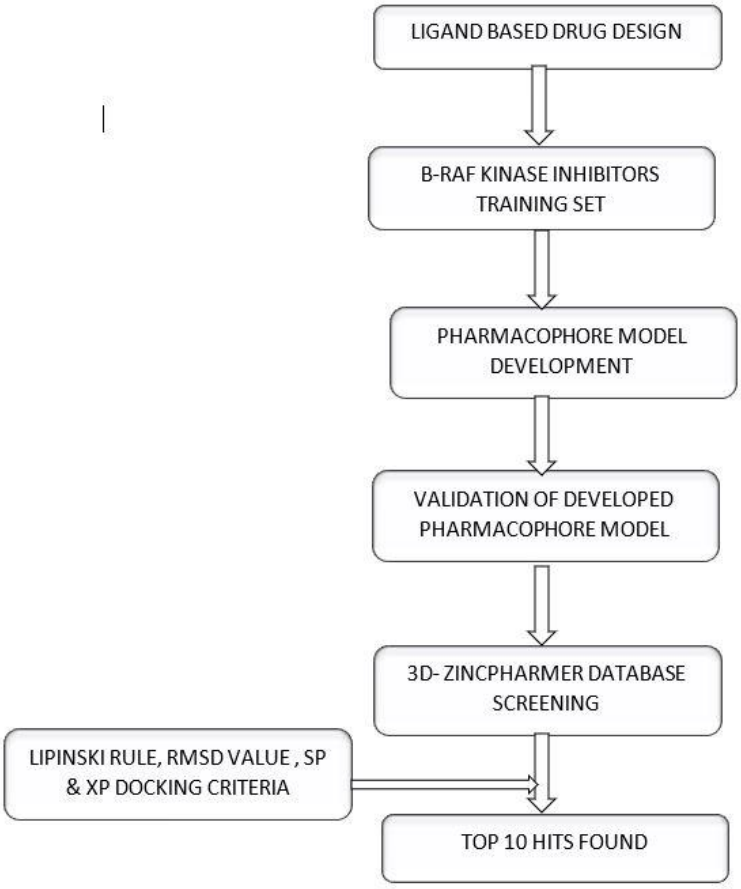

Figure 3 Schematic diagram of pharmacophore development process. LBDD - ligand-based drug design.

Molecular docking

From the protein data bank, the x-ray crystal structures of B-Raf V600E (PDB ID:3IDP) & B-Raf WT (PDB ID: 1UWH) were downloaded (https://www.rcsb.org/). By applying the OPLS 2005 force field, the downloaded proteins were subjected to the protein preparation process, review and modification, refinement, optimization, and minimization using the protein preparation step. Using GLIDE 5.6, around the active site of the proteins, a receptor grid was generated by limiting the Vander Waals scale to 0.9 to

exclude the ligand molecule from grid generation [19]. Finally, by adopting extra precision (XP)mode, all the ligands were docked in a phased manner. 10×10×10 A^0 was fixed as the grid box dimensions. For energy minimization, 800 poses per ligand were picked out of 5,000 poses per ligand obtained during the starting phase of the molecular docking process. The dielectric constant of 2.0, minimization steps to 100 was taken as limits during the energy minimization process.

Prime/MMGBSA calculations

An approach that uses a continuum solvent representation is MM/GBSA (Molecular Mechanics with Generalized Born Surface Area). Nowadays, simulations using molecular dynamics are very expensive computationally. Thereupon MM/GBSA for calculating binding free energies is utilized as it is relatively inexpensive. Then binding free energies for the top 10 hits obtained from XP docking were calculated by MM/GBSA using Prime available in the Schrodinger suite. Using the OPLS-2005 force field, the complex energies were calculated for the dock poses obtained from glide and minimized from Prime. The relative binding free energy, ΔGbind, was estimated by the equation as follows:

ΔGbind = G complex-[Gligand(unbound)+ Greceptor(unbound)]
= ΔEMM+ ΔGsolv+ ΔGSA

ΔEMM is the difference in energy between the protein-ligand complex and the sum of the protein's energies with and without ligand, ΔGsolv is the difference in GBSA solvation energy of the protein-ligand complex and the total of the solvation energies for the unliganded protein and the ligand. ΔGSA is the difference in the protein-ligand complex's surface energy and the sum of surface area energies of ligand and unliganded protein [20]. The model used in Prime MM/GBSA calculations was VSGB 2.0. It equals the solvation-free energy with an optimized tacit model [21]. During MM/GBSA calculations, the interior and exterior dielectric constants were restricted to 1 and 80, respectively. Polarization and hydrophobic terms are used to depict polar and non-polar solute-solvent concentrations in the VSGB model. This can be projected by the equation:

$$G_{pol} = \frac{1}{2}\left(\frac{1}{\sum_{in}(ij)} - \frac{1}{\sum_{sol}}\right)\sum_{i<j}\frac{q_i q_j}{f_{GB}}$$

Where fGB stands for a function of generalized Born radii (αi and Equation j) and distance between 2 atoms (ij) [22].

Result and discussion

Detection of pharmacophore model

PharmaGist is an open-source web server (https://bioinfo3d.cs.tau.ac.il/PharmaGist/) used for pharmacophore detection. A pharmacophore is the 3-dimensional arrangement of various features that allows a ligand to interact with the target protein in a specific binding pocket. The input of set of ligands along with the pivot molecule (in 3D confirmations) in the PharmaGist program will give a list of Pharmacophore candidates based on 3-dimensional superimposition of input ligand conformations that share it. The selected pivot molecule sorafenib(4-[4-[[4-chloro-3-(trifluoromethyl) phenyl] carbamoyl amino]phenoxy]-N-methylpyridine-2-carboxamide; 4-methyl benzene sulfonic acid) have benzene and pyridine rings. Various benzene and pyridine based commercially available drug molecules were randomly selected and their 3D structures were retrieved from PubChem database (https://pubchem.ncbi.nlm.nih.gov/) in SDF format. Further the ligands were imported into Marvin viewer and saved in Tripos mol2 format. Then the individual mol2 files are compressed as single zip file and submitted as a query in PharmaGist in order to identify the pharmacophore candidates [23]. Based on the score retrieved by the pairwise alignment in the PharmaGist server, the best 4 ligands were selected. The pairwise alignment and structures with the lead sorafenib of the opted ligands, the bond angles and bond distances are given in (**Figures 3** and **4**), respectively.

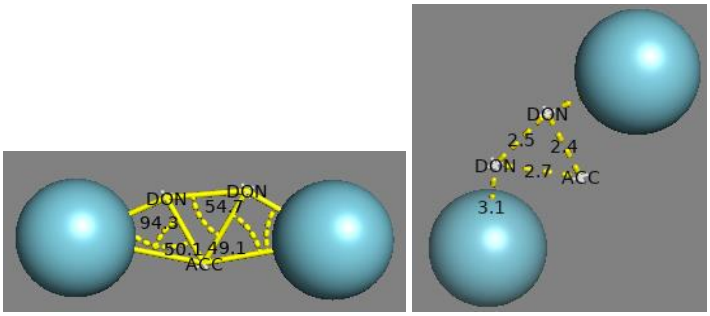

Bond angles **Bond distance**

Figure 4 Illustrating the bond angles and bond distances of selected pharmacophore model.

Table 2 Pharmacophoric characteristics of selected ligands.

Lead (Pivot molecule)	Ligand	Score	Features	Spatial features	Aromatic	Hydrophobic	H-B Donor	H-Acceptor
Sorafenib	Regorafenib	23.812	11	11	3	1	3	4
Sorafenib	Donafenib	27.78	11	11	3	1	3	4
Sorafenib	N-Desmethyl sorafenib	27.78	10	10	3	0	3	4
Sorafenib	Sorafenib	27.78	12	10	2	1	6	3

Table 3 Detailed Information on generated pharmacophore models from PharmaGist tool.

Pharmacophore model	Score of Pharmacophore model	Total features of Pharmacophore model	Aromatic Ring	Hydrophobic	H-Bond Donor	H-Bond Acceptor
1	27.78	5	2	0	2	1
2	27.78	5	2	0	2	1
3	27.78	6	1	0	3	2
4	23.812	5	1	0	2	2
5	23.812	5	1	0	2	2
6	23.812	5	1	0	2	1
7	19.843	4	1	0	2	1
8	19.843	4	1	0	2	1
9	19.843	4	1	0	2	1
10	19.843	3	2	0	0	1

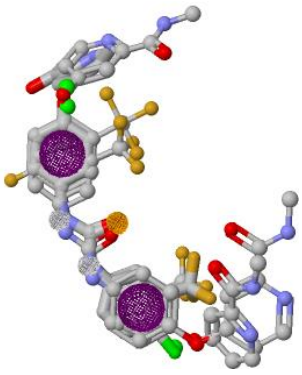

PM1

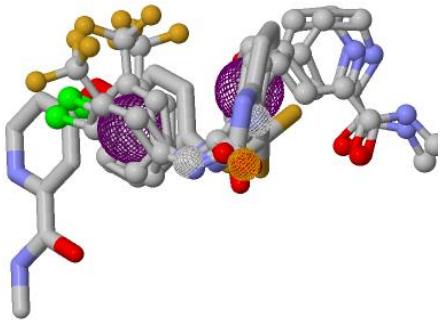

PM2

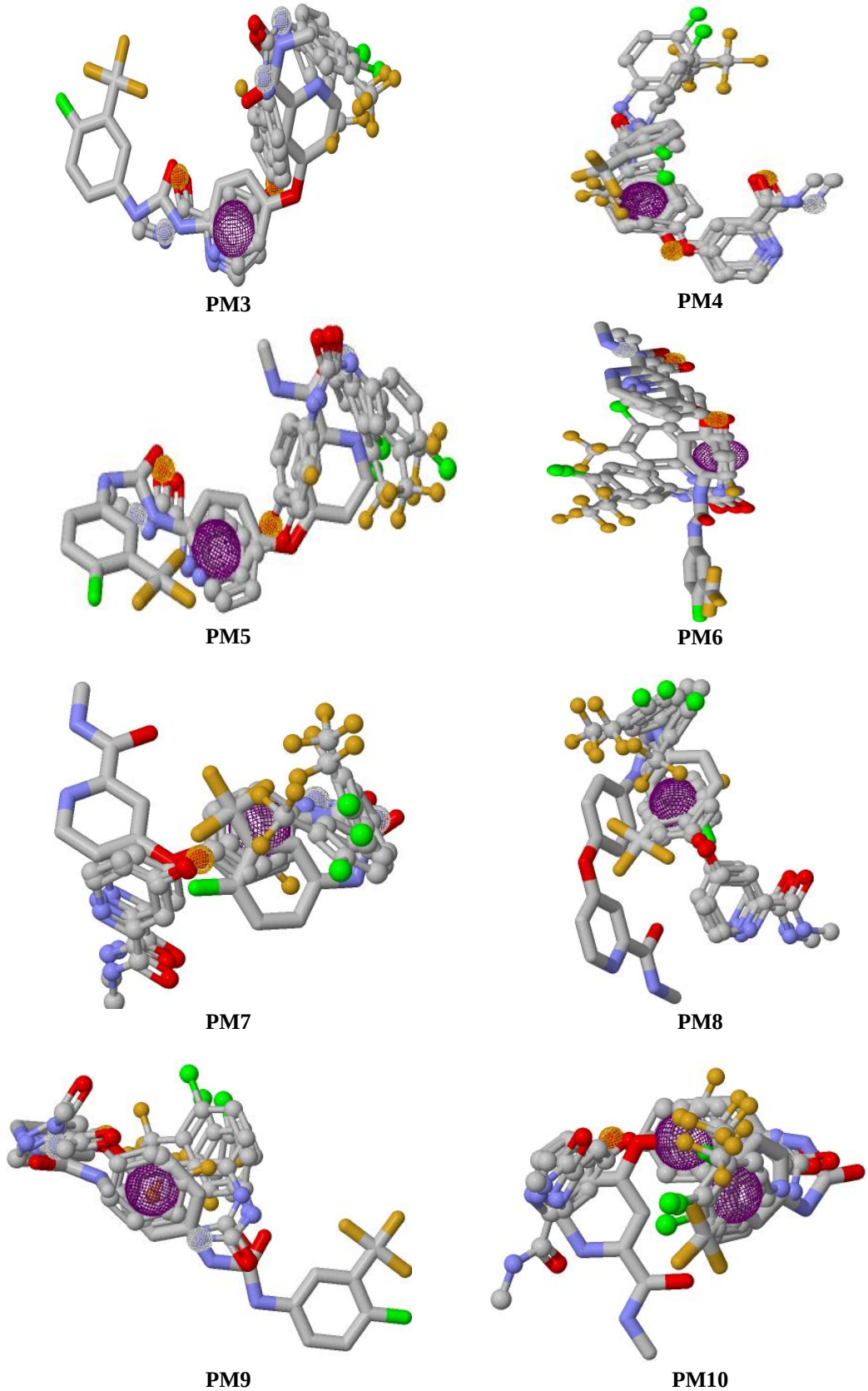

Figure 5 Pairwise-alignment of Sorafenib and selected ligands Pharmacophore models (PM1 TO PM10) are represented as ball and stick models. ■ Aromatic ■ Hydrogen bond acceptor ■ Hydrogen bond donor.

Virtual screening

The output pharmacophore model PM1 was obtained as mol2 file through PharmaGist software which has the highest score of 27.780 was submitted as a query to ZINCPharmer web server to visualize the alignment of standard with the ligands [24]. It is a 5-point pharmacophore having features of 1 hydrogen bond acceptors, 2 hydrogen bond donors & 2 aromatic rings. Inspite of Pharmacophore model PM3 having the same score as PM1, we have selected PM1 because all the input ligand molecules were aligned in a proper way where as in PM3 one ligand is not properly aligned [25]. From over 22,724,825 ligands, virtual screening process retrieved 9,47,488 hits, which are matched with the features in query pharmacophore model [26,27]. Then by applying filters of Lipinski rule, RMSD & rotatable bonds, SP & XP docking, finally we selected top 10 hits. Further theses 10 hits were subjected to molecular docking, Prime MM/GBSA calculations and ADME properties detection.

Table 4 Details of the ten molecular hits obtained using the top scoring B-Raf kinase-inhibitors.

S. No	Compound Id	RMSD	MASS	Rotatable bonds
1	ZINC68860435	0.35	396	6
2	ZINC63746558	0.304	490	4
3	ZINC48193330	0.349	369	6
4	ZINC15777616	0.319	344	6
5	ZINC72728265	0.349	315	5
6	ZINC63746843	0.349	372	4
7	ZINC33009614	0.349	482	3
8	ZINC28048642	0.322	423	3
9	ZINC02853810	0.35	381	4
10	ZINC33130204	0.35	345	3

Table 5 Details of top 10 hits.

S. No	Compound Id	RMSD	MASS	Rotatable bonds
1	ZINC68860435	0.35	396	6
2	ZINC63746558	0.304	490	4
3	ZINC48193330	0.349	369	6
4	ZINC15777616	0.319	344	6
5	ZINC72728265	0.349	315	5
6	ZINC63746843	0.349	372	4
7	ZINC33009614	0.349	482	3
8	ZINC28048642	0.322	423	3
9	ZINC02853810	0.35	381	4
10	ZINC33130204	0.35	345	3

Molecular docking

The x-ray crystal structures of B-Raf V600E (PDB ID:3IDP) & B-Raf WT (PDB ID: 1UWH) were downloaded from the protein data bank (https://www.rcsb.org/). and prepared by using the protein preparation wizard, available in GLIDE 5.6 (Schrödinger LLC,2010). OPLS_2005 force field was used for energy minimization of the crystallized ligand. Grid box was generated at a centroid of active site. The pivot molecule sorafenib and 3 input ligand molecules (Regorafenib, N-desmethyl sorafenib & Donafenib) and the obtained 10 hit molecules from zinc database were sketched in Chemdraw & saved in mol 2000 format. Then these molecules were imported into the Maestro build panel and accordingly optimized using LigPrep module (Glide 5.6). The OPLS_2005 force field was used for optimization of low energy conformer of the ligand [28]. For docking, low energy conformations of all the compounds were docked into the active site of both proteins i.e, 3IDP & 1UWH using Glide in extra precision mode without applying any constraints. The method of evaluating the accuracy of a docking procedure is to resolve how closely the lowest binding conformation predicted by the object scoring function.[29].

For all these 14 molecules the docking scores above 7 were taken into consideration. During this exercise, from the obtained 10 hits having Zinc IDs ZINC63746558, ZINC 63746843, ZINC 02853810 have glide scores as in the range of the pivot molecule when docked with the mutated B-Raf V600E protein (PDB ID:3IDP) whereas with wild type B-Raf WT protein (PDB ID :1UWH) having Zinc IDs

ZINC68860435, ZINC15777616, ZINC72728265, ZINC33009614, ZINC28048642, ZINC02853810, ZINC33130204 respectively have glide scores in the range nearer to the standard molecule i.e., Sorafenib. Finally, ZINC02853810 is common for both wild and mutant protein. Consequently, ZINC02853810 can absolutely behave as powerful inhibitors against B-Raf kinase.

Among the 10 leads, ZINC 48193330 did not exhibit satisfactory glide score and binding energy value, thereby its values are not shown in the table. Then all these molecules were subjected to Prime MMGBSA calculations i.e., binding energy analysis. The results of docking are shown in **Table 6**.

Binding free energy calculations

The Prime MMGBSA values of the top 10 hits retrieved from the Zinc database and the input ligands along with the pivot molecule, are depicted in **Table 6**. All of them exhibited satisfactory binding free energy values in the range of -71.498Kcal/mol to -113.078 Kcal/mol.

Table 6 B-Raf kinase Inhibitors, which have been employed as an Input Query for Pharmacophore Generation and hits retrieved illustrating the glide scores and binding energy values with mutated protein (PDB ID:3IDP).

S.NO	Molecule	Structure	Glide score (Kcal/mol)	Binding energy (Kcal/mol)
1	Sorafenib	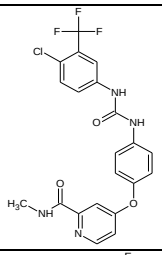	–8.892	–109.474
2.	Donafenib	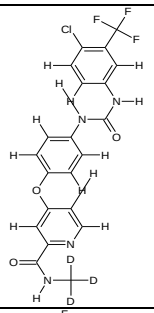	–8.822	–109.377
3.	N-Desmethyl sorafenib	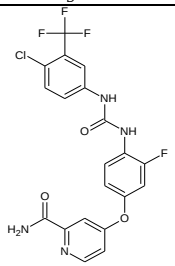	–10.224	–102.238
4.	Regorafenib	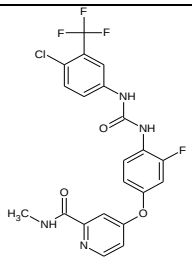	–9.683	–111.089
5.	Zinc63746558	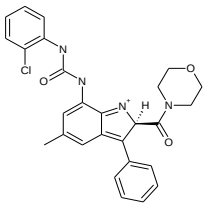	–8.175	–84.318

6.	Zinc63746843	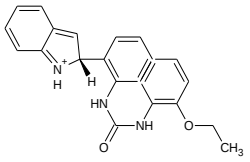	–7.655	–80.877
7.	Zinc02853810	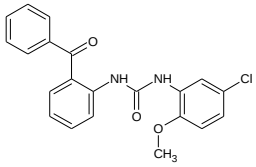	–7.962	–82.364

Table 7 B-Raf kinase Inhibitors, which have been Employed as an Input Query for Pharmacophore Generation and the hits retrieved illustrating the glide scores and binding energy values with wild type protein (PDB ID:1UWH).

S.NO	Molecule	Structure	Glide score (Kcal/mol)	Binding energy (Kcal/mol)
1.	Sorafenib	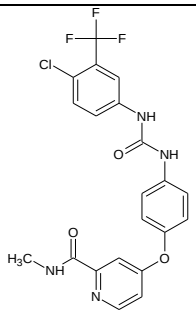	–10.450	–110.673
2.	Donafenib	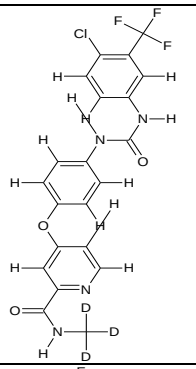	–10.546	–110.944
3.	N-Desmethyl sorafenib	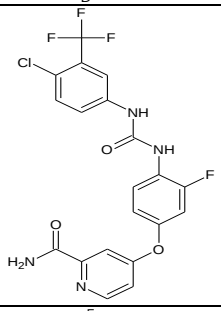	–10.107	–106.004
4.	Regorafenib	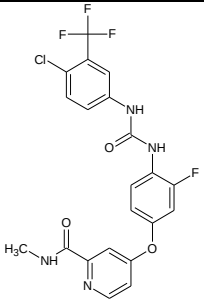	–10.953	–113.078

S.NO	Molecule	Structure	Glide score (Kcal/mol)	Binding energy (Kcal/mol)
5.	Zinc68860435	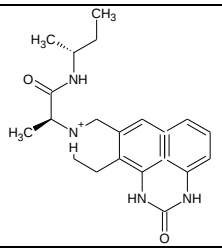	–8.497	–83.749
6.	Zinc15777616	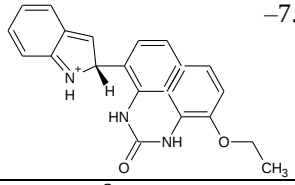	–7.421	–79.167
7.	Zinc72728265	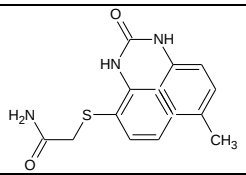	–7.355	–73.134
8.	Zinc33009614	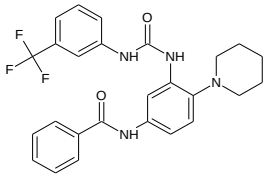	–7.126	–77.720
9.	Zinc28048642	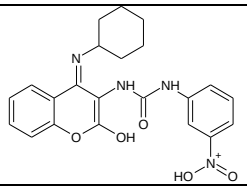	–7.615	–82.072
10.	Zinc02853810	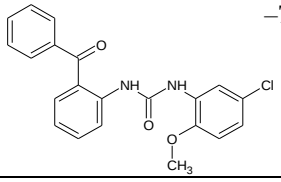	–7.624	–80.819
11.	Zinc33130204	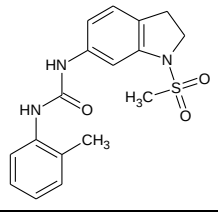	–7.636	–71.498

Interaction studies of screened hits

To analyze the interactions of hits obtained from screening, Ligand interaction diagram (LID) accessible in Schrodinger was selected. The outcomes are shown in (**Figure 6**). The pink-colored lines indicate hydrogen bond interactions. The ligand interactions are same for both B-Raf proteins. At first, the pivot molecule tangled with B-Raf kinase was explored with the aid of LID. The result is illustrated in (**Figure 6**). It exhibited 1 polar hydrogen bond interaction with Asp594, 1 polar hydrogen bond interaction with Cys532, and 2 hydrophobic interactions with Glu501.The hits retrieved from the Zinc database portrayed polar hydrogen bond interactions with Asp594, Cys532, Phe595, Leu597, hydrophobic interactions with Glu501. Among these hits, Donafenib showed 1 polar hydrogen bond interaction with Cys532, 1 polar hydrogen bond interaction with Asp594 and 2 hydrophobic interactions with Glu501. Regorafenib exhibited 1 polar hydrogen bond interaction with Cys532, 1 polar hydrogen bond interaction

with Asp594 and 2 hydrophobic interactions with Glu501. N-desmethyl sorafenib showed 2 polar hydrogen bond interactions with Cys532, 1 polar hydrogen bond interaction with Asp594 and 1 hydrophobic interaction with Glu501.ZINC48193330 portrayed 1 polar hydrogen bond interaction with Asp594, 2 hydrophobic interactions with Glu501 and 1 hydrophobic interaction with Asp594. ZINC72728265 showed 1 polar hydrogen bond interaction with Phe595, 1 polar hydrogen bond interaction with Asp594 and 2 hydrophobic interactions with Glu501. ZINC15777616, ZINC33009614, ZINC28048642 Showed 3 interactions. ZINC15777616 showed 1 polar hydrogen bond interaction with Asp594 and 2 hydrophobic interactions with Glu501. ZINC33009614 portrayed 2 polar hydrogen bond interactions with Leu597 and 1 polar hydrogen bond interaction with Phe595. ZINC28048642 exhibited 1 polar hydrogen bond interaction with Asp594 and 2 hydrophobic interactions with Glu501.ZINC68860435, ZINC02853810, ZINC33130204 showed 2 interactions. ZINC68860435 portrayed 1 polar hydrogen bond interaction with Asp594 and 1 polar hydrogen bond interaction with Cys532. ZINC02853810 showed 2 polar hydrogen bond interactions with Asp594. ZINC33130204 exhibited 1 polar hydrogen bond interaction with Cys532 and 1 polar hydrogen bond interaction with Phe595. ZINC63746843 exhibited 1 polar hydrogen bond interaction with Asp594 whereas ZINC63746558 did not show any interactions. Thereby it is clear that these molecules can act as good inhibitors against B-Raf kinase.

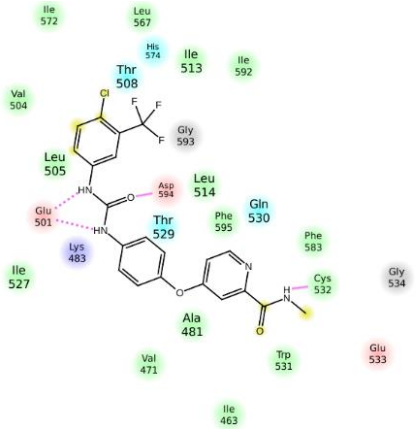

SORAFENIB

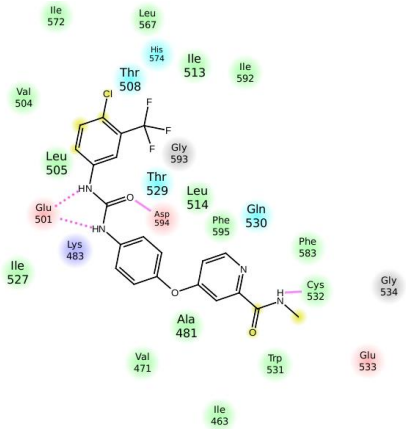

DONAFENIB

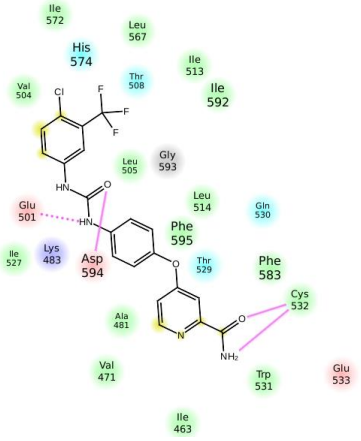

N-DESMETHL SORAFENIB

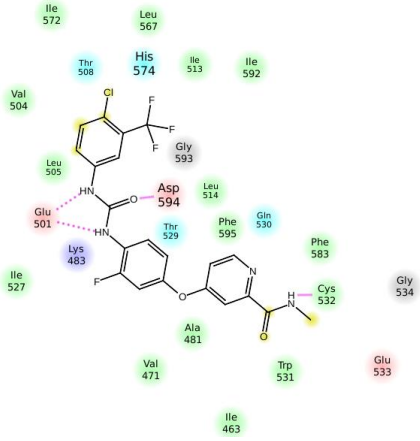

REGORAFENIB

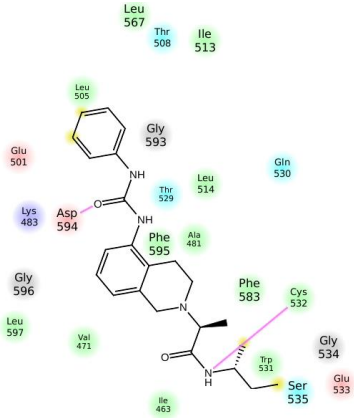

ZINC68860435

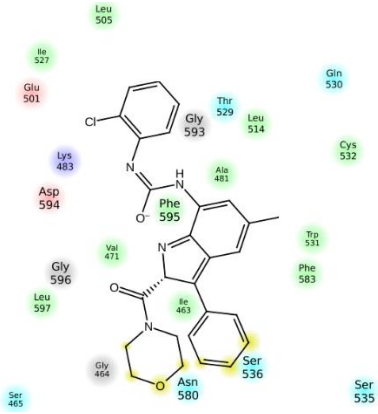

ZINC63746558

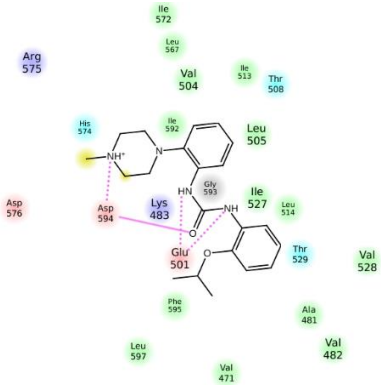

ZINC48193330

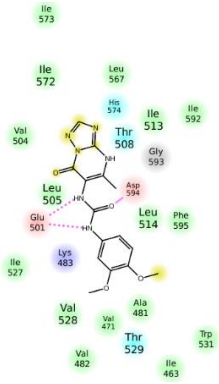

ZINC15777616

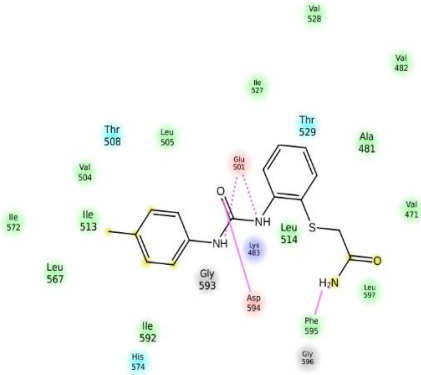

ZINC72728265

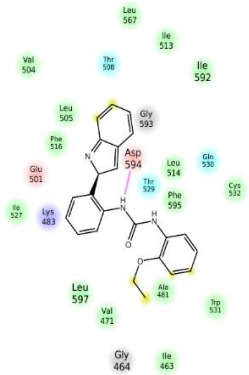

ZINC63746843

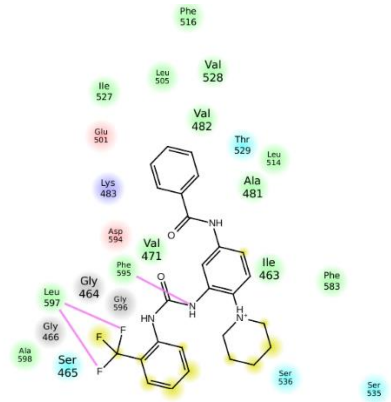

ZINC33009614

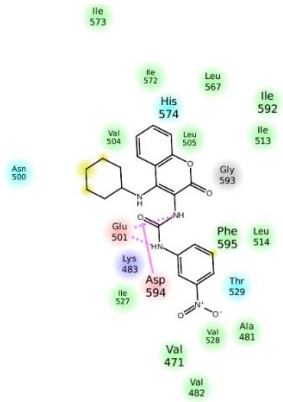

ZINC28048642

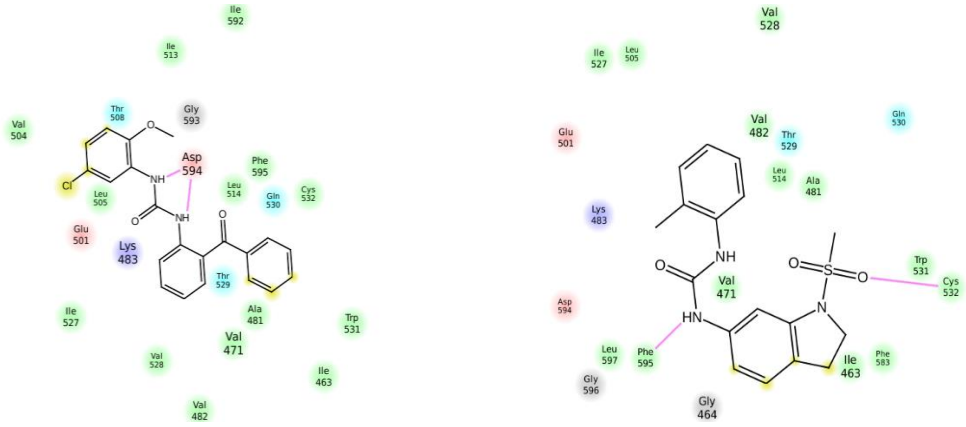

ZINC02853810 ZINC33130204

Figure 6 Ligand interaction diagrams of retrieved hits with both wild type and mutated proteins.

Prediction of ADME properties

By applying Qik Prop module of Schrodinger, ADME properties of newly designed inhibitor molecules and screened hits were computationally estimated by employing Lipinski's rule of 5. Partition coefficient (QPlogPo/w), QPlogS, QPlogHERG, QPlogBBB, Percentage Human oral absorption parameters have been established for the selected compounds [30]. All these pharmacokinetic properties were found to be satisfactory.

Table 8 ADME Properties of B-Raf kinase Inhibitors, which have been Employed as an Input Query for Pharmacophore.

S.NO	Compound	MOL.WT	QPlogPo/w	QPlogHERG	QPlogBBB	%HOA	Lipinski rule of 5
1.	Sorafenib	464.8	4.106	–5.799	–0.973	95.79	0
2.	Donafenib	464.8	4.097	–5.805	–0.987	95.590	0
3.	N-Desmethyl sorafenib	450.8	3.072	–5.556	–1.523	80.445	0
4.	Regorafenib	482.8	4.324	–5.605	–0.813	100	0
5.	ZINC68860435	394.5	2.791	–4.868	–0.414	82.49	0
6.	ZINC63746558	488.9	4.666	–2.902	–0.561	93.78	0
7.	ZINC15777616	344.3	0.758	–4.231	–1.479	70.69	0
8.	ZINC72728265	315.3	1.306	–3.192	–1.046	74.41	0
9.	ZINC63746843	371.4	4.064	–4.164	–0.130	100	0
10.	ZINC33009614	482.5	5.591	–6.240	–0.253	100	1
11.	ZINC28048642	422.4	2.914	–4.569	–1.690	79.47	0
12.	ZINC02853810	380.8	4.264	–4.365	–0.321	100	0
13.	ZINC33130204	345.4	2.125	–4.675	–0.966	86.47	0

a. Predicted octanol/water partition coefficient log P (Acceptable range –2.0 to 6.5).
b. QPlogHERG[b] (below –5)
c. Predicted Blood Brain Barrier permeability (Acceptable range –3 to 1.2)
d.%HOA: Percentage of human oral absorption (Acceptable range: <25 is poor and >80 % is high).

Conclusions

The current research aimed at identifying potent inhibitors against B-Raf kinase. To accomplish this purpose, various computational tools like molecular docking, Pharmacophore-based virtual screening, and binding free energy analysis were hired [31,32]. A 5-point common pharmacophore hypothesis (ADDRR) was established by taking 4 B-Raf kinase inhibitors and developed a pharmacophore model PM1 in which all the input ligands were properly aligned(R-H) and was viable to screen the ZINC database. The retrieved hits were docked into both B-Raf kinase's active site and further exposed to Prime MM/GBSA Calculations and ADME Properties determination. The results betrayed that the compound ZINC02853810 may act as a powerful inhibitor against both wild and mutant type B-Raf kinase as it has highest glide scores than the Standard and also had specified pharmacophoric features according to the developed PM1 model. In light of findings as mentioned earlier, it can afford few insights to the scholars in future to identify and design new molecules with potent B-Raf kinase inhibitory activity.

Acknowledgments

The authors are thankful to the Principal, Management of Sarojini Naidu Vanita Pharmacy Maha Vidyalaya, Osmania University, Hyderabad, India for providing research facilities. We gratefully acknowledge Schrodinger LLC, New York for providing us the software. We wish to express our gratitude to Department of Chemistry, Osmania University for providing facilities to carry out the research work.

References

[1] A Vivek, MD Kar and BS Kumar. PI3K/Akt/mTOR and Ras/Raf/MEK/ERK signaling pathways inhibitors as anticancer agents: Structural and pharmacological perspectives. *Eur. J. Med. Chem.* 2016; **10**, 314-41.

[2] UG Bhat, PA Zipfel, DS Tyler and AL Gartel. Novel anticancer compounds induce apoptosis in melanoma cells. *Cell Cycle*. 2008; **7**, 1851-5.

[3] S Dubey and A Roulin. Evolutionary and biomedical consequences of internal melanins. *Pigment Cell Melanoma Res*. 2014; **27**, 327-38.

[4] V Dembitsky and A Kilimnik. Anti-melanoma agents derived from fungal species. *Mathews J. Pharm. Sci*. 2016; **1**, 002.

[5] Y Yu-Shun, Z Fei, T Dan-Jie, Y Yong-Hua and Z Hai-Liang. Modification, biological evaluation and 3D QSAR studies of novel 2-(1,3-Diaryl- 4,5-Dihydro-1H-Pyrazol-5- yl) phenol derivatives as inhibitors of B-Raf Kinase. *PLoS One* 2014; **9**, e95702.

[6] AB Umar, A Uzairu, GA Shallangwa and S Uba. In silico evaluation of some 4-(quinolin-2- yl) pyrimidin-2-amine derivatives as potent V600E-BRAF inhibitors with pharmacokinetics ADMET and drug-likeness predictions. *Futur. J. Pharm. Sci*. 2020; **61**, 1-10.

[7] A Vivek, MD Kar and BS Kumar. K-Ras and its inhibitors towards personalized cancer treatment: Pharmacological and structural perspectives. *Eur. J. Med. Chem.* 2017; **125**, 299-314.

[8] T Knight and JAE Irving. Ras/Raf/MEK/ERK pathway activation in childhood acute lymphoblastic leukaemia and its therapeutic targeting. *Front. Oncol*. 2014; **160**, 1-10.

[9] HB El-Nassan. Recent progress in the identification of BRAF inhibitors as anti-cancer agents. *Eur. J. Med. Chem*. 2014; **72**, 170-205.

[10] A Nourry, A Zambon, L Davies, I Niculescu-Duvaz, HP Dijkstra, D Me´nard, C Gaulon, D Niculescu-Duvaz, BMJM Suijkerbuijk, F Friedlos, HA Manne, R Kirk, S Whittaker, R Marais and CJ Springer. BRAF inhibitors based on an imidazo[4, 5]pyridin-2- one scaffold and a meta substituted middle ring. *J. Med. Chem*. 2010; **53**, 1964-78.

[11] PTC Wan, MJ Garnett, SM Roe, S Lee, D Niculescu-Duvaz, VM Good, CM Jones, CJ Marshall, CJ Springer, D Barford and R Marais. Mechanism of activation of the RAF-ERK signaling pathway by oncogenic mutations of B-RAF. *Cell* 2004; **116**, 855-67.

[12] A Yong, W Shao-Teng, C Tang, S Ping-Hua and S Fa-Jun ong. 3D-QSAR and docking studies on pyridopyrazinones as BRAF inhibitors. *Med. Chem. Res*. 2011; **20**, 1298-317.

[13] W Lu, Z Qing, Z Gaoyuan, Z Zhang, Y Zhi, L Zhang, T Mao, X Zhou, Y Chen, T Lu and W Tang. Design, synthesis and evaluation of derivatives based on pyrimidine scaffold as potent Pan-Raf inhibitors to overcome resistance. *Eur. J. Med. Chem*. 2017; **15**, 3455-65.

[14] K Zoi, G Evripidis and PI Poulikakos. New perspectives for targeting RAF Kinase in human cancer. *Nat. Rev. Cancer*. 2017; **17**, 679-91.

[15] W Lu, Z Gaoyuan, Z Qing, C Duan, Y Zhang, Z Zhang, Y Zhou, T Lu and W Tang. Rational design, synthesis, and biological evaluation of Pan-Raf inhibitors to overcome resistance. *Eur. J. Med. Chem*. 2017; **15**, 3455-65.

[16] W Yang, Ya Chen, X Zhou, Y Gu, W Qian, F Zhang, W Han, T Lu and W Tang. Design, synthesis and biological evaluation of bis-aryl ureas and amides based on 2-amino-3-purinylpyridine scaffold as DFG-out B-Raf kinase inhibitors. *Eur. J. Med. Chem*. 2015; **89**, 581-96.

[17] PS Reddy, SS Kanth and M Vijjulatha. Discovery and design of new PI3K inhibitors through pharmacophore-based virtual screening, molecular docking, and binding free energy analysis. *Struct. Chem*. 2018; **29**, 1753-66.

[18] S Usha. Pharmacophore-based database searching of kinase-inhibitor mimetic molecular hits. *J. Bio. Innov*. 2016; **5**, 446-63.

[19] RA Friesner, JL Banks and RB Murphy. Glide: A new approach for rapid, accurate docking and scoring. 1. Method and assessment of docking accuracy. *J. Med. Chem*. 2004; **47**,1739-49.

[20] PS Reddy, SS Kanth and M Vijjulatha. Molecular dynamics and MM/GBSA integrated protocol probing the correlation between biological activities and binding free energies of HIV-1 TAR RNA inhibitors. *J. Biomol. Struct. Dyn*. 2018; **36**, 486-503.

[21] J Li, R Abel, K Zhu, Y Cao, S Zhao and RA Friesner. The VSGB 2.0 model: a next generation energy model for high resolution protein structure modeling. *Proteins* 2011; **79**, 2794-812.

[22] WC Still, A Tempczyk, RC Hawley and T Hendrickson. Semi analytical treatment of solvation for molecular mechanics and dynamics. *J. Am. Chem. Soc*. 1990; **112**, 6127-9.

[23] SA Starosyla, GP Volynets, VG Bdzhola, AG Golub, MV Protopopov and SM Yarmoluk. ASK1 pharmacophore model derived from diverse classes of inhibitors. *Bioorg. Med. Chem. Lett.* 2014; **24**, 4418-23.

[24] O Dror, DS Duhovny, Y Inbar, R Nussinov and JH Wolfson. Novel approach for efficient pharmacophore-based virtual screening: Method and applications. *J. Chem. Inf. Model.* 2009; **49,** 2333-43.

[25] S Sivaraj, RA Siva, M Karunagaran, K Yuvaraj, M Ismail, V Muralidharan, S Rangaraj and A Suguna. Bedaquiline: A potential inhibitor of COVID-19 main protease based on molecular docking. *Int. J. Res. Pharmacol. Pharmacother.* 2020; **9**, 136-144.

[26] R Zainab, A Kaleem, BM Ponczek, R Abdullah, M Iqtedar and CD Hoessli. Finding inhibitors for PCSK9 using computational methods. *PLoS One* 2021; **16**, 1-18.

[27] R Agrawal, P Jain and SN Dikshit. Ligand-based pharmacophore detection, screening of potential gliptins and docking studies to get effective antidiabetic agents. *Comb. Chem. High Throughput Screen.* 2012; **15**, 849-76.

[28] S Sivaraj, RA Siva, M Karunagaran, K Yuvaraj, M Ismail, V Muralidharan, S Rangaraj and A Suguna. Bedaquiline - A potential inhibitor of COVID-19 main protease based on molecular docking. *Int. J. Res. Pharmacol. Pharmacother.* 2020; **9**, 136-44.

[29] B Srilata, I Ramesh, S Sree Kanth and M Vijjulatha. Rational design of methicillin resistance staphylococcus aureus inhibitors through 3D-QSAR, molecular docking and molecular dynamics simulations. *Comput. Biol. Chem.* 2018; **73**, 95-104.

[30] V Tamalapakula, SK Balabadra, RK Munnaluri and V Manga. InSilico Design: Those accentuate assembly of HIV-1 capsid. *Nov. Appro. Drug Des. Dev.* 2017; **2**, 555600.

[31] K Kalpana, SR Kumar and N Ravindra. Identification of novel anti-cryptosporidial inhibitors through a combined approach of pharmacophore modeling, virtual screening, and molecular docking. *Inform. Med. Unlocked* 2021; **24**, 100583.

[32] EC Padilha, RB Serafim, DYR Sarmiento, CF Santos, CBR Santos and CHTP Silvab. New PPARα/γ/δ optimal activator rationally designed by computational methods. *J. Braz. Chem. Soc*. 2016; **27**, 1636-47.